Hindawi
Advances in Materials Science and Engineering
Volume 2019, Article ID 2189761, 8 pages
https://doi.org/10.1155/2019/2189761

Research Article

Structural Design of Partitioned Stator Doubly Salient Permanent Magnet Generator for Power Output Improvement

Warat Sriwannarat, Apirat Siritaratiwat, and Pirat Khunkitti

Department of Electrical Engineering, Faculty of Engineering, Khon Kaen University, Khon Kaen 40002, Thailand

Correspondence should be addressed to Pirat Khunkitti; piratkh@kku.ac.th

Received 31 October 2018; Revised 3 March 2019; Accepted 12 March 2019; Published 1 April 2019

Academic Editor: Georgios I. Giannopoulos

Copyright © 2019 Warat Sriwannarat et al. This is an open access article distributed under the Creative Commons Attribution License, which permits unrestricted use, distribution, and reproduction in any medium, provided the original work is properly cited.

Partitioned stator doubly salient permanent magnet generators (PS-DSPGs) have been extensively used for electrical generation mainly due to their high reliability, high electromotive force (EMF), and high-power output. Therefore, we aim to improve the output power of a PS-DSPG by designing the optimal configuration of generator pole structure. Electrical characteristics including the magnetic flux linkage distribution, phase EMF, cogging torque, voltage regulation, and power output profile were characterized by using the finite element method. After optimizing the generator pole structure including the angle of air gap arc width, it was found that the proposed PS-DSPG with 18/15 (stator/rotor) pole structure with optimized air gap arc width could produce higher EMF of about 23.24% than a conventional structure because this structure has the suitable number of pole structures. Also, an analysis of voltage regulation and power output profiles under the loaded condition were carried out, and it was indicated that the PS-DSPG based on the suitable 18/15-pole structure could provide the best machine performance where the output power is 11.63% higher than the conventional structure. Hence, the proposed PS-DSPG with 18/15-pole structure can appropriately be utilized for electrical generation, especially in low-speed operated generator applications.

1. Introduction

Permanent magnet (PM) machines with Nd-Fe-B magnet have been extensively researched for electrical generation applications because of their remarkable characteristics, such as no field excitation copper loss and robust construction [1, 2]. These properties typically result in high reliability, electromotive force (EMF), and power output of the machines [3]. The PM machines can be categorized into three types, i.e., flux reversal PM (FRPM) machine, switched-flux PM (SFPM) machine, and doubly salient PM (DSPM) machine [4–6]. Remarkably, the DSPM structures have been extensively applied in an electric vehicle and wind turbine applications since these particular structures have many advantages over other PM machine types such as wide range of operating speed and direct drive [11, 12]. The structure of a DSPM machine is developed from the traditional structure of a switched reluctance brushless machine. The DSPM structure consists of an armature winding equipped at the stator, a rotor without excitation winding, and PMs mounted at the stator yoke. The significant configuration of this machine is that the stator and rotor are salient pole, which results in high robustness, high reliability, and low-speed operation [7–10].

Lately, there are many literatures reporting that electrical characteristics indicating the performance of DSPM machines, such as magnetic flux linkage, EMF, output power, and electromagnetic torque, can be improved by using the partitioned stator (PS) technique [13–15]. More recently, the novel PS-DSPM structure for improving the performance of machines have widely been proposed, most of them contain the PM and armature winding at the stator to reduce the magnetic deterioration of PM [16].

In order to develop the PS-DSPM structure to be applied in low-speed applications, the key parameters of a general electrical machine include the yoke diameter, winding coil turn, stack length, and pole configuration [17–19]. As widely indicated in many latest literatures, the configuration of the pole in PS-DSPM structures is an influential factor related to the machine characteristics, i.e., the controlling of speed range and the output power [20–23].

Then, the aim of this work is to improve the output power of PS-DSPM by designing the generator pole configuration. The generator characteristics including the magnetic flux distribution, flux linkage, phase EMF, cogging torque, voltage regulation, and power output profiles under the loaded condition of this generator type were characterized. The simulation results were obtained using the finite element method.

2. Machine Design: Topology Selection

The conventional of PS-DSPM structures with 12/8 and 12/10 (stator/rotor) poles were initiated by Wu [15]. There are two stators in the PS-DSPM structure which are outer stator with concentrated armature winding and inner stator containing PM with Nd-Fe-B material, where the number of PM is equal to the number of outer stator pole. The rotor iron pieces installed between two stators have no PM and winding coil, and this configuration results in low weight and low inertia properties of PS-DSPM structure.

An example of the cross-sectional perspective of three-phase PS-DSPG with 6/5 and 18/15-pole structures are indicated in Figure 1(a). The number of stator/rotor poles is normalized into the $6n/5n$ stator/rotor-pole ratio where n is an integer. In this work, the stator/rotor-pole ratio is varied from $n = 1$ to 5 for analysing machine characteristics. It is noted that the thickness of PM mounted inside the stator pole is obtained by a consideration of arc between PM and core edge, θ_{apc}, which is fixed at 2.2 mechanical degrees for all proposed structures, as indicated in Figure 1(b). Also, the arcs of the air gap including the arc of the air gap outer stator tooth, θ_{aost}, the arc of the air gap outer stator tip, θ_{aot}, the arc of the air gap rotor outer edge, θ_{aro}, and the arc of the air gap rotor inner edge, θ_{ari}, are linearly introduced in each structure. The design parameters of $6n/5n$-pole PS-DSPG structure are detailed in Table 1.

In the analysis of machine characteristics, five proposed PS-DSPG structures were designed by varying the number of stator/rotor poles based on the $6n/5n$-pole ratio. Then, the magnetic flux distribution, flux linkage, and electromotive force (EMF) analysis of those structures were characterized with different rotor positions. The influence of air gap arc variation, including θ_{aost}, θ_{aot}, θ_{aro}, and θ_{ari}, on the output voltage of the machines, were also determined. Furthermore, the generator output profile under the load condition involving the voltage regulation and power output was additionally examined. The simulations were based on the 2-dimensional finite element method.

3. Results and Discussion

3.1. Magnetic Field Distribution Analysis. The magnetic field distribution at 0 electrical degrees of the proposed PS-DSPG structures consisting of 6/5, 12/10, 18/15, 24/20, and 30/25-pole was precisely analysed, as shown in Figures 2(a)–2(e), respectively. It was obviously observed that the magnetic field distribution of all PS-DSPG structures was circulated in certain parts of these structures. As indicated in Figure 2(a), the magnetic field of 6/5-pole structure is mainly circulated through four teeth of the outer stator at the lower part of the structure. The magnetic field of the 12/10-pole configuration is circulated through four outer stator teeth but in two different locations. Also, the magnetic field of the rest structures, including 18/15, 24/20, and 30/25-pole structures, is circulated through four outer stator teeth in three, four, and five different positions of those configurations, respectively. From the results, it was found that the number of circulations was equal to the number of n for all structures, which could be concluded that the characteristic of circulated magnetic field distribution depends on the number of pole structure. So, the results of magnetic field distribution will be further utilized in the discussions on phase flux linkage and EMF.

3.2. Phase Flux Linkage and EMF Analysis. The open-circuit phase flux linkage of the proposed PS-DSPG structures was calculated by integration of magnetic vector potential. As seen in Figure 3(a), the phase flux linkage of five proposed configurations is evaluated at different rotor positions, while the peak value of those flux linkage waveforms is summarized in Figure 3(b). It is seen that a variation of generator pole structure results in a change of magnetic flux linkage. The smallest flux linkage was found to be 3.62 mWb for 6/5-pole structure, whereas the highest flux linkage was 11.32 mWb for 12/10-pole structure. From the results, it was found that the flux linkage was increased with increasing the number of stator/rotor poles from $n = 1$ to $n = 2$, and then it continually decreased when increasing the pole number from $n = 3$ to $n = 5$. The explanation for a flux linkage variation with altering the number of poles can be described by the behaviour of magnetic flux circulation through the machine structure. Normally, the outer stator teeth area is considered as an area for magnetic flux circulation. As seen in the flux linkage distribution shown in Figure 2, an increase in the number of pole typically results in a reduction of the magnetic vector potential circulation area. Then, the magnitude of magnetic flux linkage becomes increasingly small as the number of pole increased. Nonetheless, the reason that 6/5-pole structure indicates the smallest flux linkage is because of an asymmetrical flux linkage distribution in this structure.

The no-load phase EMF of five proposed PS-DSPG structures was calculated by using Faraday's law of Maxwell equations. The line EMF and phase EMF are produced from five proposed PS-DSPG configurations at different rotor positions, as shown in Figures 4(a) and 4(b), respectively. Both of line and phase EMFs produce a similar trend with varying number of pole. The maximum value of EMF is summarized in Figure 4(c). It is seen that the EMFs of 18/15, 24/20, and 30/25-pole structures have a similar waveform except that of 12/10-pole having a small attenuated magnitude. The minimum EMF occurs at 6/5-pole structure due to its asymmetrical structure. Especially, the maximum EMF value of 5.61 V is found in 30/25-pole proposed structure which is about 25.27% higher than the conventional structure. As indicated in Figure 4(c), the peak value of EMF is significantly increased from $n = 1$ to $n = 3$, and afterward, it tends to be gradually stable with increasing

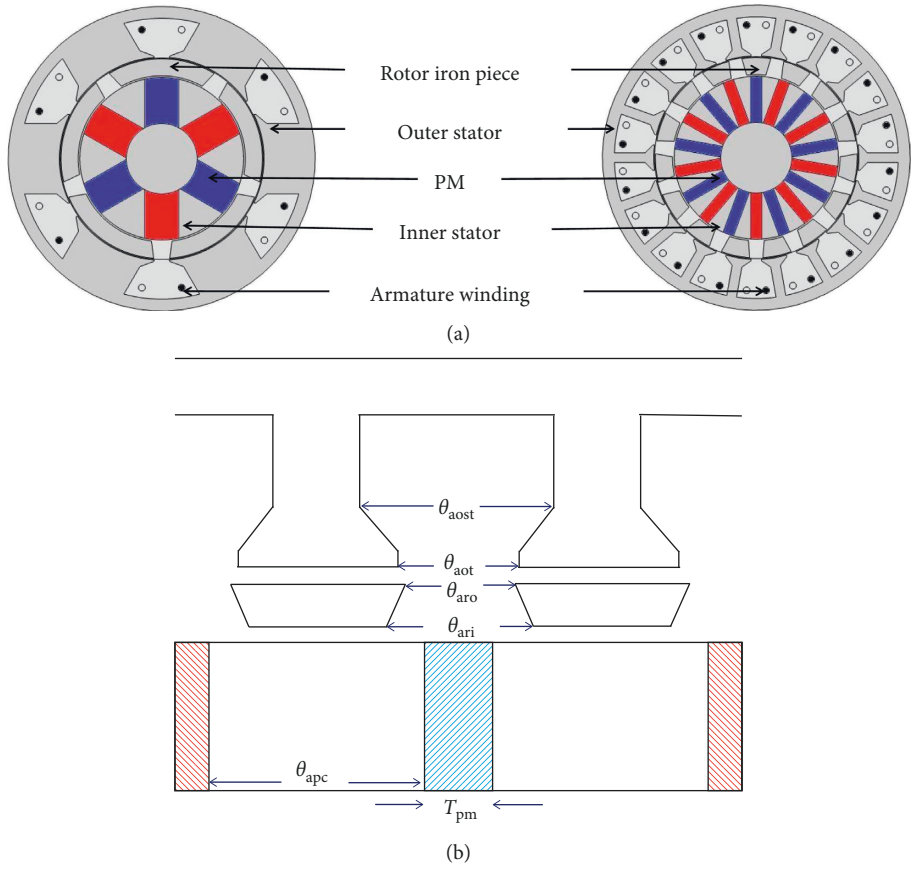

Figure 1: (a) Cross section of three-phase PS-DSPG with 6/5 and 18/15 (stator/rotor) poles. (b) Parameter design of the proposed PS-DSPG structures.

Table 1: The design parameters of $6n/5n$-pole PS-DSPG structure.

Parameter	$n = 1$	$n = 2$	$n = 3$	$n = 4$	$n = 5$
Rotor iron piece number, N_r	5	10	15	20	25
The number of PM, N	6	12	18	24	30
Rated rotor speed (rpm)			400		
Diameter of coil (mm)			0.4		
The number of coils, N_c			18		
Outer radius of outer stator, R_{oso} (mm)			45		
Inner and outer air gap width, g (mm)			0.5		
Yoke radius of outer stator, R_{osy} (mm)			41.5		
Inner radius of outer stator, R_{osi} (mm)			30		
Outer radius of inner stator, R_{ro} (mm)			24		
Inner radius of inner stator, R_{isi} (mm)			10.4		
Arc between PMs at core, θ_{apc} (degree)			2.2		
PM thickness, T_{pm} (mm)	10	5	3.2	2.3	1.77
Arc of air gap outer stator tooth, θ_{aost} (degree)	19.5	17	14.5	12	9.5
Arc of air gap outer stator tip, θ_{aot} (degree)	8.25	7	5.75	4.5	3.25
Arc of air gap rotor outer edge, θ_{aro} (degree)	9.175	8.34	7.505	6.67	5.835
Arc of air gap rotor inner edge, θ_{ari} (degree)	14.125	12.5	10.875	9.25	7.625

the number of pole. In general, the EMF magnitude depends on flux-linkage motion through the generator structure. Regarding to different proposed PS-DSPG structures, it is indicated that when the structures modified by increasing the number of pole, the total space for flux linkage movement through each structure becomes larger. As a result, the EMF enhancement is demonstrated.

From the results, it is seen that the 18/15, 24/20, and 30/25-pole structures could provide the EMF in a similar range. When comparing the suitability between these structures, the 18/15-pole structure has the smallest quantity of generator pole for producing the EMF in this range. The less quantity of generator normally indicates more robustness of the structure. Then, the 18/15-pole PS-DSPG structure is

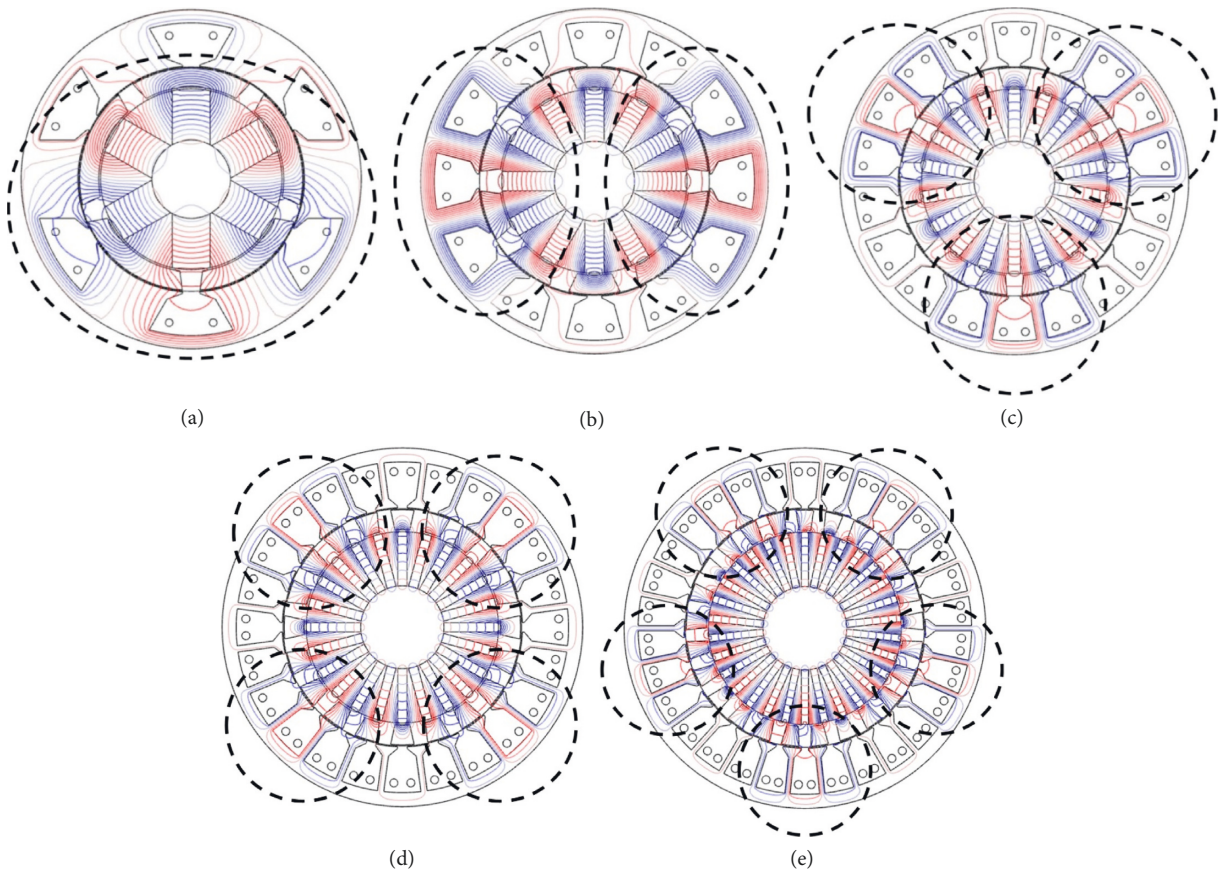

Figure 2: Open-circuit magnetic field distributions at 0 degrees of (a) 6/5, (b) 12/10, (c) 18/15, (d) 24/20, and (e) 30/25-pole PS-DSPG structures.

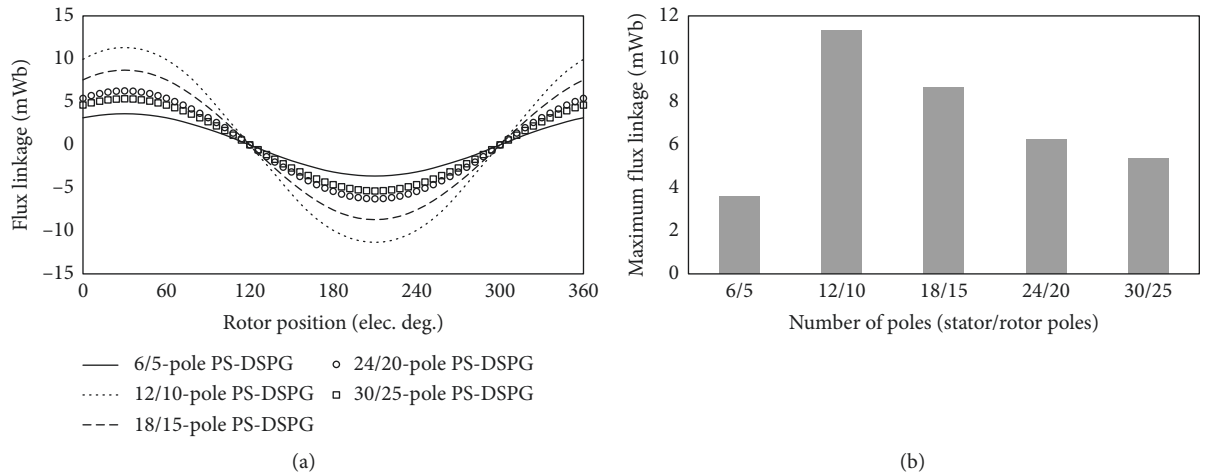

Figure 3: Open-circuit phase flux linkage of the proposed PS-DSPG structures (a) at various rotor positions. (b) The maximum value of each structure.

selected as the most suitable structure in this work since it could produce high EMF with the appropriate number of stator and rotor poles. The EMF produced from this structure is 5.49 V which is about 21.06% higher than the conventional structure. In addition, in order to improve the electrical performance of PS-DSPG, the air gap arc width of each proposed structure will further be optimized. Additionally, the initial cogging torque characteristic of all proposed PS-DSPG structure will be further examined in order to estimate pole configuration variation.

3.3. Initial Cogging Torque Analysis. Cogging torque of PS-DSPG structure generally acts as the initial torque required

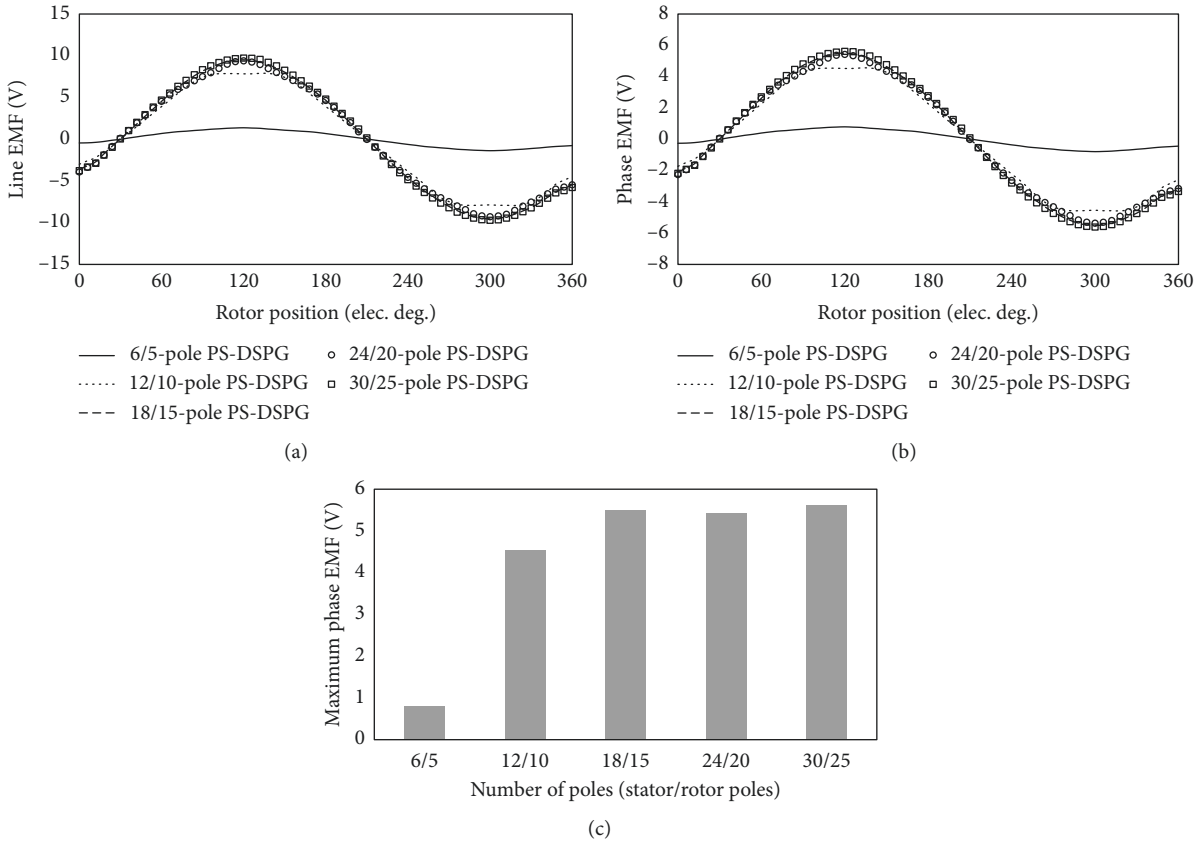

Figure 4: Open-circuit of proposed PS-DSPG structures: (a) line EMF, (b) phase EMF at various rotor positions, and (c) phase EMF indicating the maximum value of each structure.

to start the generator. In this model, the cogging torque is calculated by the magnetic field generated from the inner stator pole flowing through the rotor iron piece towards the outer stator slot. Figure 5 indicates the initial cogging torque waveform of the five proposed PS-DSPG structures. It is obviously noticed that the cogging torque of 6/5-pole has a high-symmetrical value because the cross section of magnetic field has the larger area than those in other proposed structures. The cycle of the cogging torque waveform of 30/25-pole configuration is significantly larger than the other proposed structures because of a very short length between adjacent rotor pieces. The 12/10 and 24/20-pole structures indicate symmetrical cogging torque with the small magnitude due to their suitable pole configuration. Moreover, the 18/15-pole PS-DSPG structure has an asymmetrical cogging torque waveform, while this structure produced smaller cogging torque compared with other proposed structures and also the conventional structure. It was found that the 18/15-pole PS-DSPG structure produces the cogging torque 56.79% lower than conventional structure.

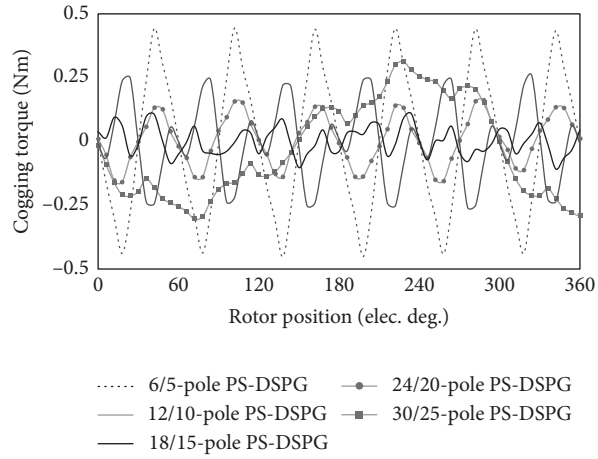

Figure 5: Cogging torque of the proposed PS-DSPG structures at various rotor positions.

3.4. Influence of Air Gap Arc Width Variations. In addition, in order to improve the electrical performance of PS-DSPG, the air gap arc width of each proposed structure is optimized. The suitable angles of air gap arc width of five proposed PS-DSPG structures, consisting of θ_{aost}, θ_{aot}, θ_{aro}, and θ_{ari}, were optimized in addition. An influence of θ_{aot}, θ_{aro}, and θ_{ari} on the phase voltage under no-load condition of the proposed structures was investigated. It was found that θ_{aot}, θ_{aro}, and θ_{ari} have a negligible impact on the phase EMF. However, θ_{aost}, which is the air gap arc between two outer stator teeth, plays a significant effect on the phase voltage of proposed PS-DSPG structures except in the 6/5-pole structure. Figure 6 indicates the phase voltage of five proposed PS-DSPG structures versus the percentage angle of

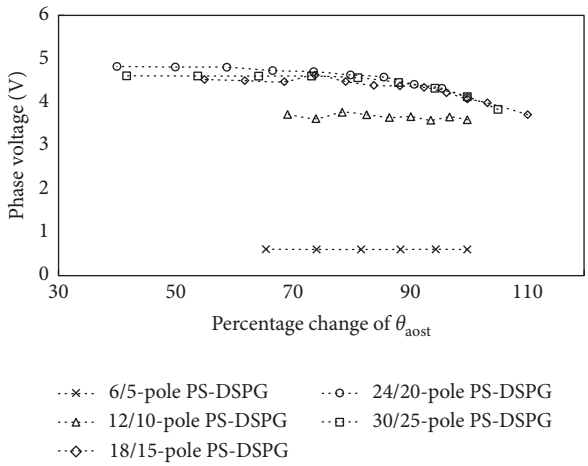

Figure 6: Open-circuit phase voltage of the proposed PS-DSPG structures with the percentage change of θ_{aost}.

θ_{aost} compared to the initial configuration. The conventional value of θ_{aost}, which refers to one hundred percent scale, is shown in Table 1.

It is seen that the phase voltage of 12/10, 18/15, 24/20, and 30/25-pole structures tends to be improved when θ_{aost} is reduced from 110% to approximately 73% of an initial value. Then, it gradually becomes stable at θ_{aost} below 73%. For 6/5-pole structure, θ_{aost} has no impact on the phase voltage. According to the PS-DSPG structure, an angle of θ_{aost} is directly related to a voltage induction area at outer stator teeth. The narrower angle of θ_{aost} normally provides a larger area for producing the voltage, which results in higher total phase voltage. When reducing θ_{aost} less than 73%, angle of θ_{aost} has no impact on the phase voltage because each structure has enough area for producing the voltage from a derivative of flux linkage.

For 6/5-pole structure, an area for voltage induction is much bigger than its desired area, so θ_{aost} has no impact on phase voltage produced by this asymmetrical structure. However, the other air gap arcs, which are θ_{aot}, θ_{aro}, and θ_{ari}, have no impact on the voltage because these parameters have insignificant impact on voltage induction area in these PS-DSPG structures. In addition, it is noted that the structure that has a narrower angle of θ_{aost} that normally yields small area for winding coil at the outer stator. We found that a winding coil area is linearly reduced according to a decrease in θ_{aost}. Consequently, a suitable value of θ_{aost} for each structure is selected by a beginning point of phase voltage saturation, which is about 65–73% for 18/15-pole structure and 65%–73% for 12/10, 24/20, and 30/25-pole structures. From this result, it is concluded that the EMF of 18/15-pole PS-DSPG structure with optimized air gap arc width is 23.24% improved from the conventional structure.

Additionally, the characteristics of five optimal modified structures in load condition will be further investigated in order to verify the suitable PS-DSPG structure.

3.5. Voltage Regulation and Output Power Analysis. The voltage regulation and output power of all optimized PS-DSPG structures were concurrently analysed under load condition at 18 turns of winding coil. The voltage regulation is a relationship waveform between an optimized phase voltage and load current of each proposed structure. The quality of voltage regulation depends on an equilibrium between phase voltage and load current of each proposed structure. It is noted that the maximum load current is determined by using the optimized phase voltage value of each proposed structure, which is obtained from Figure 6. From the voltage regulation result indicated in Figure 7(a), it is seen that when load current increased, the phase voltage of five proposed structures is reduced with different consequences. When the number of pole increased, the load current range of each structure is decreased due to an increase in resistance of coil. Then, the widest load current range is found for 12/10-pole structure, which could be useful to adapt in several load applications. Meanwhile, the 24/20-pole structure could provide the highest phase voltage magnitude.

To characterize the power output, the phase voltage and load current at each point of voltage regulation result are multiplied. The characteristic of power output of each proposed PS-DSPG structure is shown in Figure 7(b). The phase voltage of each current value in this graph can be known from the voltage regulation result. The power output of each structure increases until the middle range of voltage regulation waveform, and afterwards, it decreases. It is generally known that the highest output power could be obtained from the middle range of the voltage regulation waveform of each structure. In Figure 7(b), it is remarkably shown that the 18/15-pole structure can produce the highest power output, following 12/10, 24/20, 30/25, and 6/5, respectively. The power output produced by 18/15-pole structure is about 11.63% higher than that produced by the conventional structure. This is because the suitable pole configuration of this structure can produce higher phase voltage and wider range of load current than the other structures. Accordingly, this structure can provide the most appropriate voltage regulation and highest power output.

Finally, it can be summarized that the generator pole structure is an influential factor to improve performance of PS-DSPG. In our analysis, it is found that the 18/15-pole PS-DSPG structure indicates better performance than the other proposed structures since it has the suitable number of pole structure. Especially, the EMF and power output produced by this structure are classified in high range compared to other structures proposed in the literatures. Hence, the PS-DSPG with 18/15-pole structure becomes another suitable structure for low-speed range operation and can be applied for producing electrical power from renewable energy.

4. Conclusion

In this paper, the PS-DSPG was designed by optimizing the generator pole structure, which is $6n/5n$-pole ratio in order to improve the performance of the generator. The flux-linkage distribution, flux linkage, EMF, and cogging torque of all the proposed PS-DSPG structures were

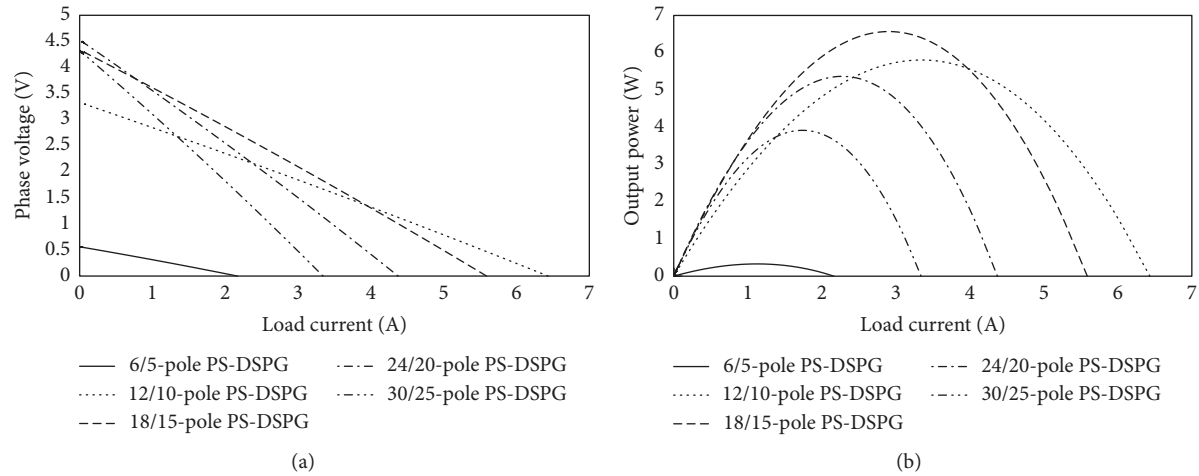

Figure 7: Output characteristics of proposed PS-DSPG structures: (a) voltage regulation and (b) output power.

investigated under the no-load condition. The voltage regulation and power output under load condition were also examined. The results showed that the configuration of the generator pole structure had a significant impact on magnetic flux circulation. Also, the flux linkage in the generator is linearly decreased when the outer stator teeth area is reduced. Especially, the results of phase EMF and cogging torque indicates that the 18/15-pole structure is the most suitable structure due to its symmetrical configuration. After optimizing θ_{aost}, it was found that the EMF of 18/15-pole structure was improved from a conventional structure by 23.24%. Moreover, the 18/15-pole PS-DSPG structure could produce the highest power output, which is 11.63% higher than that produced by the conventional structure since the pole structure indicates effective voltage regulation. Hence, the proposed 18/15-pole PS-DSPG structure could be appropriately chosen for producing electrical power in low-speed operation regarding to renewable energy applications.

Data Availability

All data generated or used to support the findings of this study are included within the article.

Conflicts of Interest

The authors declare that there are no conflicts of interest regarding the publication of this paper.

Acknowledgments

This work was financially supported by the Thailand Research Fund (Grant no. MRG-6180010) and Khon Kaen University through research funds to support high-potential students to study and research on an expert program in the year 2016 (Grant no. 591JT211). The authors would also like to thank the Department of Mechanical Engineering, Khon Kaen University, for COMSOL software facility.

References

[1] S. M. Hosseini, M. Agha-Mirsalim, and M. Mirzaei, "Design, prototyping, and analysis of a low cost axial-flux coreless permanent-magnet generator," *IEEE Transactions on Magnetics*, vol. 44, no. 1, pp. 75–80, 2008.

[2] Z. Q. Zhu and D. Howe, "Electrical machines and drives for electric, hybrid, and fuel cell vehicles," *Proceedings of the IEEE*, vol. 95, no. 4, pp. 746–765, 2007.

[3] Y. Du, C. Zou, and X. Liu, "A double-sided linear primary permanent magnet vernier machine," *Scientific World Journal*, vol. 2015, Article ID 596091, 8 pages, 2015.

[4] C. X. Wang, I. Boldea, and S. A. Nasar, "Characterization of three phase flux reversal machine as an automotive generator," *IEEE Transactions on Energy Conversion*, vol. 16, no. 1, pp. 74–80, 2001.

[5] E. Hoang, B. A. Hamid, and L. Jean, "Switching flux permanent magnet poly-phased synchronous machines," in *Proceedings of the European Conference on Power Electronics and Applications (EPE'97)*, vol. 1, Trondheim, Norway, September 1997.

[6] Y. Tang, J. J. H. Paulides, and E. A. Lomonova, "Analytical modeling of flux-switching in-wheel motor using variable magnetic equivalent circuits," *ISRN Automotive Engineering*, vol. 2014, Article ID 530260, 10 pages, 2014.

[7] Y. Liao, F. Liang, and T. A. Lipo, "A novel permanent magnet motor with doubly salient structure," *IEEE Transactions on Industry Application*, vol. 31, no. 5, pp. 1069–1078, 1995.

[8] S. Eriksson, "Inherent difference in saliency for generators with different PM materials," *Journal of Renewable Energy*, vol. 2014, Article ID 567896, 5 pages, 2014.

[9] M. Cheng, K. T. Chau, and C. C. Chan, "Design and analysis of a new doubly salient permanent magnet motor," *IEEE Transactions on Magnetics*, vol. 37, no. 4, pp. 3012–3020, 2001.

[10] M. Cheng, K. T. Chau, and C. C. Chan, "Static characteristics of a new doubly salient permanent magnet motor," *IEEE Transactions on Energy Conversion*, vol. 16, no. 1, pp. 20–25, 2001.

[11] K. T. Chau, C. C. Chan, and C. Chunhua Liu, "Overview of permanent-magnet brushless drives for electric and hybrid electric vehicles," *IEEE Transactions on Industrial Electronics*, vol. 55, no. 6, pp. 2246–2257, 2008.

[12] Y. Fan, K. T. Chau, and M. Cheng, "A new three-phase doubly salient permanent magnet machine for wind power generation," *IEEE Transactions on Industry Application*, vol. 42, no. 1, pp. 53–60, 2006.

[13] Z. Q. Zhu, Z. Z. Wu, D. J. Evans, and W. Q. Chu, "Novel electrical machines having separate PM excitation stator," *IEEE Transactions on Magnetics*, vol. 51, no. 4, pp. 1–9, 2015.

[14] D. J. Evans and Z. Q. Zhu, "Novel partitioned stator switched flux permanent magnet machines," *IEEE Transactions on Magnetics*, vol. 51, no. 1, pp. 1–14, 2015.

[15] Z. Z. Wu, Z. Q. Zhu, and J. T. Shi, "Novel doubly salient permanent magnet machines with partitioned stator and iron pieces rotor," *IEEE Transactions on Magnetics*, vol. 51, no. 5, pp. 8105212–8105223, 2015.

[16] Z. Q. Zhu, H. Hua, D. Wu, J. T. Shi, and Z. Z. Wu, "Comparative study of partitioned stator machines with different PM excitation stators," *IEEE Transactions on Industry Applications*, vol. 52, no. 1, pp. 199–208, 2016.

[17] J. T. Shi, A. M. Wang, and Z. Q. Zhu, "Influence of PM-and armature winding-stator positions on electromagnetic performance of novel partitioned stator permanent magnet machines," *IEEE Transactions on Magnetics*, vol. 53, no. 1, pp. 1–12, 2017.

[18] Z. Zhang, Y. Yan, and Y. Tao, "A new topology of low speed doubly salient brushless DC generator for wind power generation," *IEEE Transactions on Magnetics*, vol. 48, no. 3, pp. 1227–1233, 2012.

[19] R. Nor Firdaus, N. Misron, C. A. Vaithilingam, M. Nirei, and H. Wakiwaka, "Improvement of energy density in single stator interior permanent magnet using double stator topology," *Mathematical Problems in Engineering*, vol. 2014, Article ID 787382, 15 pages, 2014.

[20] Y. S. Chen, Z. Q. Zhu, and D. Howe, "Vibration of PM brushless machines having a fractional number of slots per pole," *IEEE Transactions on Magnetics*, vol. 42, no. 10, pp. 3395–3397, 2006.

[21] D. Ishak, Z. Q. Zhu, and D. Howe, "Permanent magnet brushless machines with unequal tooth widths and similar slot and pole numbers," in *Proceedings of the Conference Record of the 2004 IEEE Industry Applications Conference, 2004. 39th IAS Annual Meeting*, vol. 2, Seattle, WI, USA, October 2004.

[22] T. Sun, J.-M. Kim, G.-H. Lee, J.-P. Hong, and M.-R. Choi, "Effect of pole and slot combination on noise and vibration in permanent magnet synchronous motor," *IEEE Transactions on Magnetics*, vol. 47, no. 5, pp. 1038–1041, 2011.

[23] A. S. Abdel-Khalik, "Five-phase modular external rotor PM machines with different rotor poles: a comparative simulation study," *Modelling and Simulation in Engineering*, vol. 2012, Article ID 487203, 14 pages, 2012.


The Scientific
World Journal
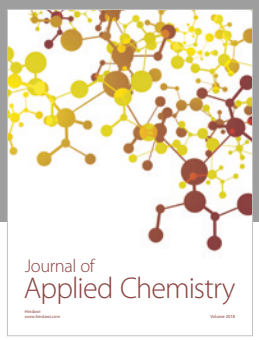
Journal of
Applied Chemistry
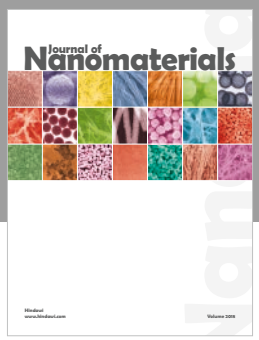
Journal of
Nanomaterials

Scientifica

International Journal of
Polymer Science
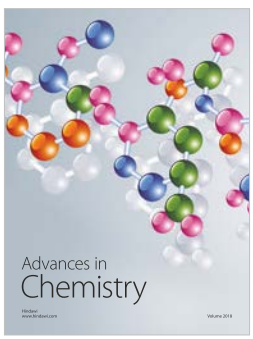
Advances in
Chemistry

Hindawi
Submit your manuscripts at
www.hindawi.com
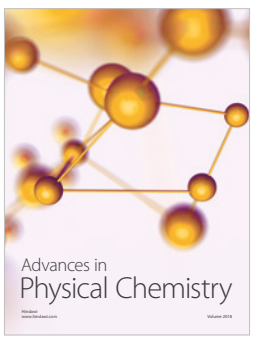
Advances in
Physical Chemistry

International Journal of
Analytical Chemistry
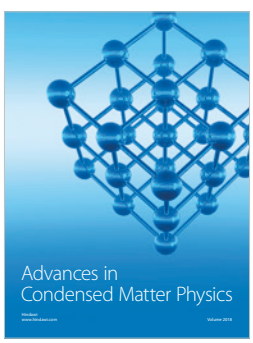
Advances in
Condensed Matter Physics
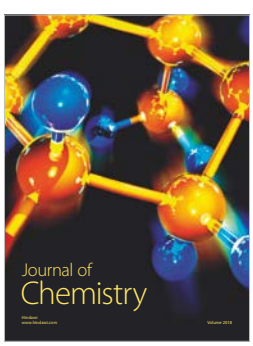
Journal of
Chemistry

International Journal of
Biomaterials
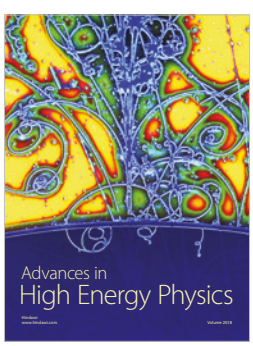
Advances in
High Energy Physics

Journal of
Engineering

Journal of
Nanotechnology

International Journal of
Corrosion

Journal of
Materials

BioMed
Research International
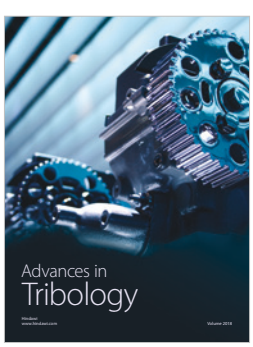
Advances in
Tribology
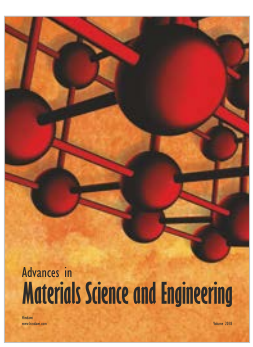
Advances in
Materials Science and Engineering